Comparison between classical potentials and ab initio for silicon under large shear

Julien Godet, Laurent Pizzagalli, Sandrine Brochard, Pierre Beauchamp

Comparison between classical potentials and ab initio for silicon under large shear

J. Godet, L. Pizzagalli, S. Brochard, P. Beauchamp

Laboratoire de Métallurgie Physique, CNRS UMR 6630, Université de Poitiers, B.P. 30179, 86962 Futuroscope Chasseneuil Cedex, France

E-mail: Laurent.Pizzagalli@univ-poitiers.fr

Abstract.

The homogeneous shear of the {111} planes along the $< 110 >$ direction of bulk silicon has been investigated using ab initio techniques, to better understand the strain properties of both shuffle and glide set planes. Similar calculations have been done with three empirical potentials, Stillinger-Weber, Tersoff and EDIP, in order to find the one giving the best results under large shear strains. The generalized stacking fault energies have also been calculated with these potentials for complementing this study. It turns out that the Stillinger-Weber potential better reproduces the ab initio results, for the smoothness and the amplitude of the energy variation as well as the localisation of shear in the shuffle set.

Submitted to: *J. Phys.: Condens. Matter*

PACS numbers: 68.47.Fg, 61.72.Lk, 02.70.Ns, 62.20.Mk

1. Introduction

Dislocations in materials generate a long-range strain field, which must be taken into account in atomistic simulations for a proper treatment of the defects. As a consequence, large systems including thousands of atoms have to be employed. Only in specific cases it is possible to use a limited number of atoms. For example, if the considered dislocations are ideally straight and infinite, the core structure may be investigated with few hundreds of atoms. Precise electronic and atomic structure calculations can then be performed using ab initio methods [1, 2, 3, 4, 5]. Still, investigating the formation, mobility or interaction of dislocations requires a large system with a few thousands of atoms [6], preventing the use of such methods. Then the atomic simulation must be performed with empirical interatomic potentials.

With such potentials, the simulations can be performed with a large number of atoms and for a long time scale, with a moderate cost in calculation time. Then, they are a valuable mean for simulating the activation of complex physical mechanisms, using techniques like molecular dynamics. However, it remains difficult to evaluate the validity of the results obtained from such studies. Interatomic potentials are built in order to reproduce with a fair accuracy a limited number of physical quantities, usually at equilibrium. The reliability of potentials is then doubtful when one investigates physical mechanisms or configurations where the atomic structure is far from its equilibrium state, such as, for example, reconstruction of surfaces, point or extended defects. Moreover, the nature of material is also an important factor. It is commonly agreed that the results obtained using interatomic potentials are qualitatively better for metals than in the case of covalent materials. This problem is very sensible for silicon in particular, since it is largely studied, for technology purposes, or as a model for semiconductors. Several kinds of potentials have been proposed but it is difficult to assess the superiority of one over the other. In particular, the transferability is poor in many cases. Several comparative studies on elastic constants, bulk point defects, core properties of partial dislocation, structure of disordered phases have already been performed with these potentials [7, 8, 9]. They conclude that, for each kind of system or physical mechanism, one must determine the best interatomic potential.

Recently, Godet *et al* [10] have studied the nucleation of dislocations from a surface step on silicon. The dislocation formation with this mechanism would explain the presence of dislocation observed in nano-materials [11] where the dimensions are too small to allow a classical multiplication mechanism like Franck- Read sources. This would also explain the appearance of dislocations from cleavage ledges, when silicon is plastically deformed at low temperature [12]. Since the observation of the very first stage of dislocation nucleation is difficult, the atomic simulation may bring up an interesting alternative. However, recently, Godet *et al* have shown that the obtained results were potential dependent [13]. During the process of nucleation of the dislocations, the atomic structure is so largely deformed that the potentials go out of their usual domain of validity, which may explain these disagreements. It would be helpful to find out which

is the silicon potential giving the best results in the case of large shears.

In this paper, an attempt is presented in view of determining the best interatomic potential for silicon submitted to large shear strain, by comparing results obtained for different potentials with ab initio calculations. First, considering homogeneous shear of bulk silicon, two criteria have been used for the potential selection. The first one bears upon the variation of the bulk energy as a function of the applied strain. The second criterion is related to atomic configurations in that it considers how imposed atomic displacements distribute between the shuffle and the glide sets of the {111} planes. In particular, we focus on the mechanism of atomic bonds switching from one neighbor to another. After the homogeneous shears, a second part is devoted to generalized stacking fault (GSF) energy surfaces, in particular their shape in both shuffle and glide set planes at large fault vectors. All these situations contribute to a better understanding of the strain properties of both glide and shuffle planes, related to the mechanisms of dislocations nucleation and mobility [14, 15, 16, 17] or to the mechanisms of cleavage and fracture of this crystal [18, 19, 20].

2. Methodology

2.1. Shear technics

In ambient conditions silicon crystallizes into the diamond cubic structure which is formed of two interpenetrated face centered cubic sublattices called in the following sublattice 1 and 2. In this structure, the dislocations glide in the {111} dense planes with a $1/2 < 110 >$ Burgers vector corresponding to the shortest vector of the fcc lattice. We have studied the silicon bulk under large shear strain, along the {111} planes in the $< 110 >$ direction, from zero up to a given shear strain allowing to recover the cubic diamond structure. As the cubic diamond structure includes two fcc sublattices, there are two kinds of {111} planes, that are alternately piled up, the narrowly spaced between the (111) planes of the sublattices 1 and 2, and the widely spaced between 2 and 1, called glide and shuffle set planes respectively [21] (figure 1). To deform the crystal, we have progressively applied shear strain increments about 4% on both sublattices 1 and 2, up to a shear strain called $\gamma_{23tot} \simeq 122\%$. This limit corresponds to the ratio of a slip in a shuffle set equal to a Burgers vector $\mathbf{b}$ ($=\mathbf{x}_3$) by the shuffle and glide set interplanar distance ($= \mathbf{x_2}/3$), i.e. $\frac{x_3}{x_2/3} = \sqrt{3}/\sqrt{2}$. After each shear increment, the atomic positions belonging to the sublattice 2 are relaxed in all directions to minimize the energy. Note that the calculations are performed at 0 K and constant volume. The aim is to monitor the energy evolution during the shear, and determine how the homogeneous shear strain is divided between the shuffle set and the glide set. In this paper, we call displacement in one set (shuffle or glide), the shift after application of the strain (before relaxation), and shear strain in one set the ratio of the displacement by the interplanar distance in this set (figure 1). Note that, interplanar distances may vary because the sublattice 2 is free. However, as the shear is done at constant volume, the addition of the shuffle and

glide set interplanar distances remains constant. For the same reason, the bulk shear stress σ_{23} is obtained by the derivation of the atomic energy curve against the applied shear strain γ_{23} .

We have also calculated the GSF energy and the restoring forces along the slip directions in shuffle and glide planes. The unrelaxed GSF energy surface is obtained by simply moving one half of the crystal rigidly with respect to the other half along a cut plane in the middle of the crystal. The GSF energy is defined as a function of the relative displacement **f** of the two atomic planes immediately adjacent to the crystal cut plane. To calculate the GSF energy with atomic and volume relaxation, the atoms in the two planes immediately adjacent to the cut plane are restricted to move along the $< 111 >$ direction only, in order to keep the relative displacement **f**, whereas the other atoms relax in all directions. Therefore, the actual relative displacement **f** might be different from the displacement between the centers of both halves of the crystal. The restoring force in a given direction, corresponds to the derivative of the GSF energy versus the displacement **f**. Here, we focused on the $< 110 >$ direction in the shuffle and glide set, and also on the $< 112 >$ direction in the glide set, since perfect dislocations can be dissociated in two Shockley partial dislocations with $1/6 < 112 >$ Burgers vectors in that set. The local shear stress required to maintain the displacement **f** in both sides of the cut plane is directly proportional to the opposite of the restoring forces.

2.2. Computational Methods

First principles calculations of the bulk shear are performed using the ABINIT package [22], the exchange correlation energy being determined within the local density approximation with the Teter Pade parametrization [23] which reproduces Perdew-Wang. The valence electron wave functions are expanded in a plane wave basis with a cut off energy of 15 Ha. The ionic potential is modeled by a norm conserving pseudo-potential from Troullier and Martins [24]. To simulate the bulk shearing process, a periodic cell orientated along $1/2[121]$ ($\mathbf{x}_1$), $[\bar{1}1\bar{1}]$ ($\mathbf{x}_2$) and $1/2[\bar{1}01]$ ($\mathbf{x}_3$) is used, including 12 atoms, i.e. 6 $\{111\}$ atomic planes (3 glide set and 3 shuffle set planes) along $\mathbf{x}_2$. For the reciprocal space integration, we have used 9 special k-points in the irreducible Brillouin zone when the cell is not sheared, and 15 special k-points when the cell is sheared owing to the reduced symmetry. The k-points lattice obtained with the Monkhorst and Pack scheme [25], is the reciprocal of the super-lattice defined by the supercell in the real space by $3\mathbf{x}_1$, $2\mathbf{x}_2$ and $5\mathbf{x}_3$, the origin of this k-point lattice being shifted by a $[0.5, 0.5, 0.5]$ vector. The SCF cycle is stopped when the difference on total energy between two successives cycles is smaller than 10^{-10} Ha. Metallic occupation of levels is allowed using the Fermi-Dirac smearing occupation scheme. The atomic positions are relaxed using the Broyden - Fletcher - Goldfarb - Shanno minimization down to forces smaller than 5×10^{-5} Ha/Bohr (2.5×10^{-3} eV/Å). We have compared our results with the ab initio study performed by Umeno *et al* [26] where the same

calculation is realized with a full relaxation of volume and ionic position but only up to 35% of strain.

For the empirical bulk shear calculations, three different interatomic potentials have been used, Stillinger-Weber (SW) [27], Tersoff [28] and the Environment-Dependent Interatomic Potential (EDIP) [29]. The pioneering potential of SW has only eight parameters and is fitted to few experimental properties of both crystallized (cubic diamond) and liquid silicon. It consists of a linear combination of two and three body terms. The Tersoff functional form is fundamentally different from the SW form in that it includes many body interactions thanks to a bond order term. As a result, the strength of individual bonds is affected by the presence of surrounding atoms. The final version called T3 has eleven adjustable parameters fitted to ab initio results for several Si polytypes. The third potential, EDIP, has a functional form similar to that of Tersoff but slightly more complicated. It incorporates several coordination-dependent functions to adapt the interactions for different coordinations. 13 parameters are determined by fitting to a fairly small ab initio database.

The dimensions of the calculation cell must be twice larger than the cut off radius of the interatomic potentials to minimize interaction of atoms with their images in neighboring cells. So a calculation cell with the same geometry as before is used, but containing 576 atoms. The relaxation of atomic positions is performed with a conjugate gradients algorithm until the magnitudes of the forces are smaller than 10^{-4} eV/Å.

The GSF energy surfaces calculations have been performed with the three interatomic potentials and we have compared our results with the GSF energy surfaces obtained with first principles calculations by Juan and Kaxiras [30, 31]. Note that several energy curves or unstable stacking fault energies have been calculated with those interatomic potentials [8, 32, 33]. Here, periodic conditions are applied only along the $< 112 >$ and $< 110 >$ directions. In the third direction, the number of {111} planes is large enough (30) to avoid spurious interactions between the free surfaces and the crystal cut plane. The system contains 1440 atoms.

3. Results / discussion

3.1. Homogeneous shear strains

The calculation of homogeneous shear strain of bulk silicon has been performed ab initio and with the three interatomic potentials. The observation of the sheared atomic structure obtained with the ab initio calculation (figure 2) shows that the strains are essentially located in the shuffle set. The bonds between atoms across the shuffle set plane are successively weaken, broken and then formed again. This is confirmed by the monitoring of the electronic density where the covalent character of the bonds progressively vanishes to reach a metallic character at half of the applied shear strain in the shear direction ($< 110 >$). Our calculation is in agreement with the ab initio study realized by Umeno *et al* [26], where it is found that the band gap is progressively closed

with the applied shear. At the maximum of the applied shear strain, each shuffle set plane have been shifted by a Burgers vector of a perfect dislocation and the diamond crystal is recovered.

To compare the different interatomic potentials, the atomic energy and the corresponding shear stresses as a function of the applied shear strain are calculated and represented in figure 3. For small strains, all the energy curves coincide and the stress curves are linear, indicating that the empirical potentials are fairly well fitted to the elastic coefficients. The shear modulus associated to $< 110 >\{111\}$ shear at constant volume obtained from the ab initio calculation is around 52 GPa close to the value calculated with volume relaxation [26] and also relatively close to the value obtained from the elastic coefficient calculated at 0 K ($C_{12} - \frac{1}{3}(2C_{44} + C_{12} - C_{11}) = 48.3$ GPa) [34]. For larger strains, the potentials may be classified in two groups depending on whether they are close or not to ab initio. SW belongs to the first group with energy curves in fair agreement with ab initio which presents smooth maxima of similar heights at half of the applied shear, whereas EDIP and Tersoff are in the other group with larger maxima and angle-shaped curves. Regarding stresses, the variations of SW and ab initio are relatively smooth compared to EDIP and Tersoff, with similar theoretical shear strengths reached at about one fourth of the total applied strain, while the ones obtained with EDIP and Tersoff are larger and reached at about half of the applied strain (table 1). Note that our ab initio theoretical shear strength at constant volume is relatively close to the value calculated with volume relaxation [26]. SW seems to be the best interatomic potential to model the shear stress evolution during the atomic bond switching. Probably the introduction of temperature would smooth the energy curves, and in the case of the Tersoff potential, would allow the crossing of the energy barrier to recover the diamond crystal. However, the general shape of calculated curves will be preserved, in particular for deformations corresponding to theoretical shear strenghs.

To analyze the atomic structure, the displacements and shear strains in both shuffle and glide set planes along the $< 110 >$ shear directions have been determined (figure 4). For applied strains up to half maximum, all potentials show a similar behavior, the displacements in the shuffle set plane following the applied strains, while those in the glide set oscillate weakly with a magnitude lower than 0.15 Å. For larger applied strains, the displacements in the shuffle set reach the Burgers vector of a perfect dislocation. In the glide set they return to zero, except for the Tersoff potential where the displacements in the shuffle set remain practically constant and where the displacements are then located in the glide set along $< 112 >$. The variations of shear strains in both planes, show that the ab initio, SW and EDIP results are relatively close to each other. The interatomic potentials modeling properly these effects are SW and EDIP.

In figure 3, the shear strains of the glide set planes are represented with dashed line next to the bulk shear stress with full line. In all cases, while most of the displacements are localized in the shuffle set, the shear strains of the glide set are approximately linear with the bulk shear stresses, with a large shear modulus (μ), for example 134 GPa with ab initio calculations. The strains localized in the glide set remain then elastic and

linear whereas those of the shuffle set do not. Moreover the large shear modulus of the glide set shows that the displacements in the glide set, although always small, play an important role on the bulk shear stress. This is confirmed by the study of Umeno [26] where it is concluded that the subtle displacements in the glide set have a remarkable effect on the shear stress.

3.2. GSF energy and restoring force

We have investigated the GSF energy surfaces and the corresponding restoring forces in directions of Burgers vectors **b**, calculated with ab initio techniques [31] and interatomic potentials, in order to compare the localized shear stresses in the shuffle and glide set planes. Two directions have been investigated $< 110 >$ in the shuffle and glide set for perfect dislocations, and $< 112 >$ in the glide set for Shockley partial dislocations.

Usually, one considers the maxima of the GSF energy, i.e. the unstable stacking fault energy γ_{us} (table 2), as an important parameter for gliding. In addition with γ_{us}, we also determine the maxima of the restoring force, τ_{max}, along the three directions (table 3). In all cases, the lowest values are obtained for the $< 110 >$ direction in the shuffle set plane, as expected. The best γ_{us} are given by Tersoff and EDIP, the SW potential tending to underestimate in the shuffle set and to overestimate in the glide set. Regarding the restoring force, the SW potential yields the best results, the large values for EDIP and Tersoff coming from the singularities in the curves. It appears that the sole determination of these maxima is not enough to discriminate between the potentials. An additional indication is given by the location of the maxima. The best agreement with ab initio is then obtained for the SW potential, with maxima in the vicinity of 0.3b, whereas for both EDIP and Tersoff, they are located at displacements greater than 0.4b.

Instead of considering only maxima, we compared directly the variations. Along the three directions, the ab initio GSF energy variations, calculated by Juan et al [31], are smooth, with sinusoidal-shaped curves. Comparing with the GSF energy for the three potentials (figure 5), the best qualitative agreement is obtained with the SW potential. Both EDIP and Tersoff show large and abrupt variations of the GSF energy, as soon as the displacement is greater than 0.4b. In particular, distorted shapes and angular points are present for EDIP in the glide set, and Tersoff in the shuffle set. If we focus on the favored glide direction for perfect dislocation, i.e. the $< 110 >$ in the shuffle set plane, it appears that the Tersoff potential shows the worst results, with a deep local minimum at 0.5b. Using EDIP and SW, instead, leads to an energy maximum at 0.5b, as obtained with the ab initio calculation. The whole EDIP and SW GSF energy curves are in fair agreement with ab initio, although the smoothest variations are obtained with SW.

More indications can be gained from the calculation of the restoring forces in the three cases. The variations, represented in figure 5, are similar to the bulk shear stress curves, shown in figure 3. The various conclusions drawn from the analysis of the

GSF energy variations remain valid here. The best agreement is obtained for the SW potential, with a rather smooth variation of the restoring force in all directions. With EDIP, discontinuous variations are obtained for displacements along $< 110 >$ in both glide and shuffle sets. In particular, the restoring force along the favored direction, $< 110 >$ in the shuffle set, increases to a large maximum just before 0.5b, and then suddenly drops to a symmetric minimum. This sharp behavior is not observed in the ab initio curve. The last potential, Tersoff, shows the worst results, with discontinuities between 0.4b and 0.6b in the shuffle set, so in the range of large deformation, but also for small displacements in the glide set.

4. Conclusion

We have investigated the properties of bulk silicon submitted to a homogeneous shear, using ab initio techniques. It appeared that the shear takes place almost entirely in the shuffle set planes, with only slight displacements in the glide set planes. The atomic bonds between atoms on both sides of the shuffle set, loose progressively their covalent character until a metallic state is established in the shear direction at half the maximum applied shear. Then the reverse process is observed, and the perfect diamond crystal structure is recovered. We have shown that glide set plays a predominant role on the bulk shear stress and that the strains localized in the glide set are linear and elastic with respect to the bulk shear stresses, with a large shear modulus. At 0 K, silicon can be viewed as formed by a stacking of 'elastic' glide set planes and 'plastic' shuffle set planes. Our results are confirmed by the analysis of GSF energy surfaces and restoring forces, determined with ab initio calculation [31], which suggests that shuffle set is the favored place for the glide event at 0 K. The variations of bulk shear stress are similar to the variations of the restoring force in the active glide plane. So at 0 K, a correct description of the restoring force is a prerequisite to model glide events.

One of the main objective of this work was the determination of the best interatomic potentials in the case of largely deformed silicon systems. We have then performed calculations of sheared bulk silicon and GSF energy surfaces with SW, Tersoff and EDIP potentials, and compared with ab initio results. For sheared bulk silicon we observed that EDIP and SW provided a faithful description of the glide event, and strains and stresses analysis showed that the theoretical shear strength is better determined with SW. Regarding the GSF energy surfaces and restoring forces, it appears that the shuffle set is the preferred place for the glide events at 0 K for all the potentials, but the best values of the restoring force (τ_{max}) is given by SW. It must also be emphasized that the smoothest description of the glide of one plane on another is also obtained with SW. In summary, under large strains, SW seems to be the best potential to model qualitatively silicon.

This work was partially motivated by a previous work on the dislocation nucleation process from a surface step under an uniaxial stress [10]. In fact, in that case, a large homogeneous shear strain is present in the atomic structure. Our results explain why it

is possible to model the nucleation process with the SW potential, whereas a potential like Tersoff leads to fracture or local amorphization under stress.

Finally, one possible explanation for the differences between the potentials, such as the discontinuities and local minima on the energy and stress, may come from the cut off radius of each potential. In fact, when the atomic structure is largely deformed, the number of atoms taken into account in the energy calculation may abruptly changes, leading to sharp energy variation. The smooth behavior of SW may then be explained by its relatively large cut off radius of 3.77Å. Another possible explanation is the simplicity of its functional form and the small number of fitted parameters. For Tersoff and EDIP, the functional is more complicated with more parameters. While this is required to model properly a large range of experimental quantities, a more complex functional may lead to non physical behaviors, when the atomic structure is far from the equilibrium state.

References

[1] Öberg S, Sitch P K, Jones R and Heggie M I 1995 *Phys. Rev.* B **51** 13138
[2] Justo J F, Fazzio A and Antonelli A 2000 *J. Phys.: Condens. Matter* **12** 10039
[3] Ewels C P, Wilson N T, Heggie M I, Jones R and Briddon P R 2001 *J. Phys.: Condens. Matter* **13** 8965
[4] Justo J F, Antonelli A and Fazzio A 2001 *Solid State Commun.* **118** 651
[5] Pizzagalli L, Beauchamp P and Rabier J 2003 *Phil. Mag.* **83** 1191
[6] Rasmussen T, Vegge T, Leffers T, Pedersen O B and Jacobsen K W 2000 *Phil. Mag.* A **80** 1273
[7] Balamane H, Halicioglu T and Tiller W A 1992 *Phys. Rev.* B **46** 2250
[8] Justo J F, Bazant M Z, Kaxiras E, Bulatov V V and Yip S 1998 *Phys. Rev.* B **58** 2539
[9] Moriguchi K and Shintani A 1998 *Jpn. J. Appl. Phys.* **37** 414
[10] Godet J, Pizzagalli J, Brochard S and Beauchamp P 2002 *Scripta Materialia* **47** 481
[11] Wu R X and Weatherly G C 2001 *Phil. Mag.* A **81** 1489
[12] Argon A S and Gally B J 2001 *Superlatt. Microstruc.* **45** 1287
[13] Godet J, Pizzagalli L, Brochard B and Beauchamp P, to be published.
[14] Duesbery M S and Joós B 1996 *Phil. Mag. Lett.* **74** 253
[15] Justo J F, Antonelli A and Fazzio A 2001 *Physica* B **302-303** 398
[16] Bulatov V V, Justo J F, Cai W, Yip S, Argon A S, Lenosky T, de Koning M. and Diaz de la Rubia T 2001 *Phil. Mag.* A **81** 1257
[17] Rabier J, Cordier P, Demenet J L and Garem H 2001 *Mater. Sci. Eng.* A **A309-A310** 74
[18] Pérez R and Gumbsch P *Acta Mater.* **48** 4517
[19] Gally B J and Argon A S 2001 *Phil. Mag.* A **81** 699
[20] Pirouz P, Demenet J L and Hong M H 2001 *Phil. Mag.* A **81** 1207
[21] Hirth J P and Lothe J 1982 *Theory of dislocations* (Wiley)
[22] The ABINIT code is a common project of the Université Catholique de Louvain, Corning Incorporated, and other contributors (URL http://www.abinit.org).
[23] Goedecker S, Teter M and Huetter J 1996 *Phys. Rev.* ,B **54** 1703
[24] Troulier N and Martins J L 1991 *Phys. Rev.* B **43** 1993
[25] Monkhorst H J and Pack J D 1976 *Phys. Rev.* B **13** 5188
[26] Umeno Y and Kitamura T 2002 *Mater. Sci. Eng.* B **B88** 79
[27] Stillinger F H and Weber T A 1985 *Phys. Rev.* B **31** 5262
[28] Tersoff J 1989 *Phys. Rev.* B **39** 5566
[29] Bazant M Z, Kaxiras E and Justo J F 1997 *Phys. Rev.* B **56** 8542
[30] Kaxiras E and Duesbery M S 1993 *Phys. Rev. Lett.* **70** 3752
[31] Juan Y M and Kaxiras E 1996 *Phil. Mag.* A **74** 1367
[32] Duesbery M S, Michel D J, Kaxiras E and Joos B 1991 *Mat. Res. Soc. Symp. Proc.* **209** 125
[33] de Koning M, Antonelli A, Bazant M Z and Kaxiras E 1998 *Phys. Rev.* B **58** 12555
[34] Karki B B, Ackland G J and Crain J 1997 *J. Phys.: Condens. Matter* **9** 8579

Table captions

Table 1. Theoretical shear strengths and strains obtained with different potentials.

Table 2. Unstable stacking fault energies γ_{us} along relevant Burgers vectors (**b**), for the shuffle and glide planes in (J/m^2), Unrelaxed (U) and Relaxed (R) with atomic and volume relaxation. (The γ_{us} is not necessarily localized at $\mathbf{f} = b/2$.)

Table 3. Maximum value of the restoring force τ_{max} for the relevant directions (in $eV/Å^3$).

	Constant volume				volume relaxation
	SW	Tersoff	EDIP	DFT-LDA	DFT-LDA [26]
Theoretical shear strength (GPa)	9.6	16.7	13.9	7.95	10
Theoretical shear strain (%)	32.7	53	53	24.5	30
(% of the applied strain)	27	43	43	20	25

Table 1

	SW		Tersoff		EDIP		DFT-LDA [31]	
	U	R	U	R	U	R	U	R
$< 110 >$ shuffle	1.38	0.83	2.57	1.50	2.16	1.32	1.84	1.67
$< 112 >$ glide	4.78	3.08	3.33	1.96	3.24	1.71	2.51	1.91
$< 110 >$ glide	26.09	6.21	31.19	5.27	13.43	6.14	24.71	$\simeq$5.55

Table 2

	SW	Tersoff	EDIP	DFT-LDA [31]
$< 110 >$ shuffle	0.055	0.144	0.160	0.093
$< 112 >$ glide	0.299	0.535	0.322	0.174
$< 110 >$ glide	0.437	0.688	1.908	0.268

Table 3

Figure captions

Figure 1. Definition of displacements and shear strains shown on a deformed structure (right) compared to the perfect lattice (left). In shuffle set planes the displacement is called D_{sh}, and the shear strain is defined as $\frac{D_{sh}}{H_{sh}}$, H_{sh} being the 'height' of the shuffle set. In glide set planes, similar notations are taken.

Figure 2. Snapshot of the bulk structure during homogeneous shear process. Here, bonds are drawn solely on the criterion of distance and are not indicative of a true chemical bonds between atoms.

Figure 3. Upper graph: variation of atomic energy during the shear process (in eV/atom). Lower graphs : bulk shear stress σ_{23} in GPa (solid line) and shear strain of the glide plane multiplied by a shear modulus in GPa (dashed line), for the different potentials.

Figure 4. The left panel shows the displacements in both shuffle (dashed line) and glide (dotted line) plane in unit b vs the applied shear strain. The solid line corresponds to the addition of shuffle and glide displacements. The right panel shows the shear strain in both shuffle (dashed line) and glide (doted line) planes vs the applied shear strain. The solid line correspond to the applied strain.

Figure 5. The fully relaxed GSF energies and the corresponding restoring force $(-\tau)$ on the shuffle (left) and glide (right) set planes (bold lines for $< 110 >$ and thin line for $< 112 >$ directions) for the three interatomic potentials.

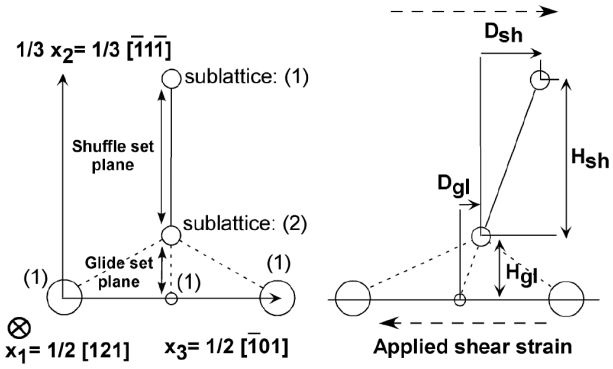
1/3 x2= 1/3 [1̄1̄1]
sublattice: (1)
Shuffle set plane
sublattice: (2)
Glide set plane
(1)
(1)
(1)
x1= 1/2 [121]
x3= 1/2 [1̄01]
Dsh
Hsh
Dgl
Hgl
Applied shear strain

Figure 1

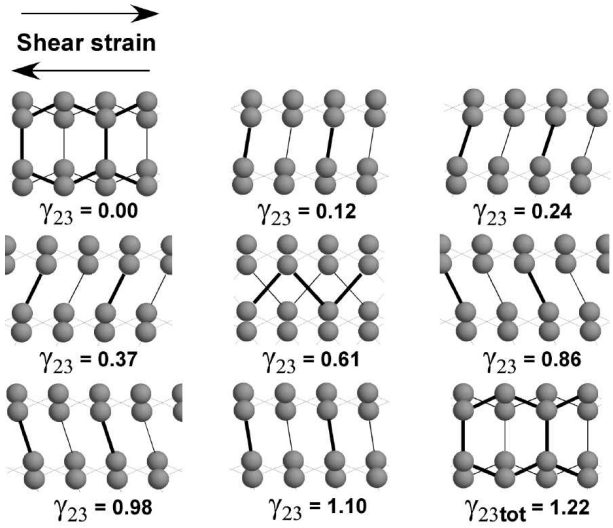
Shear strain
γ_{23} = 0.00
γ_{23} = 0.12
γ_{23} = 0.24
γ_{23} = 0.37
γ_{23} = 0.61
γ_{23} = 0.86
γ_{23} = 0.98
γ_{23} = 1.10
γ_{23tot} = 1.22

Figure 2

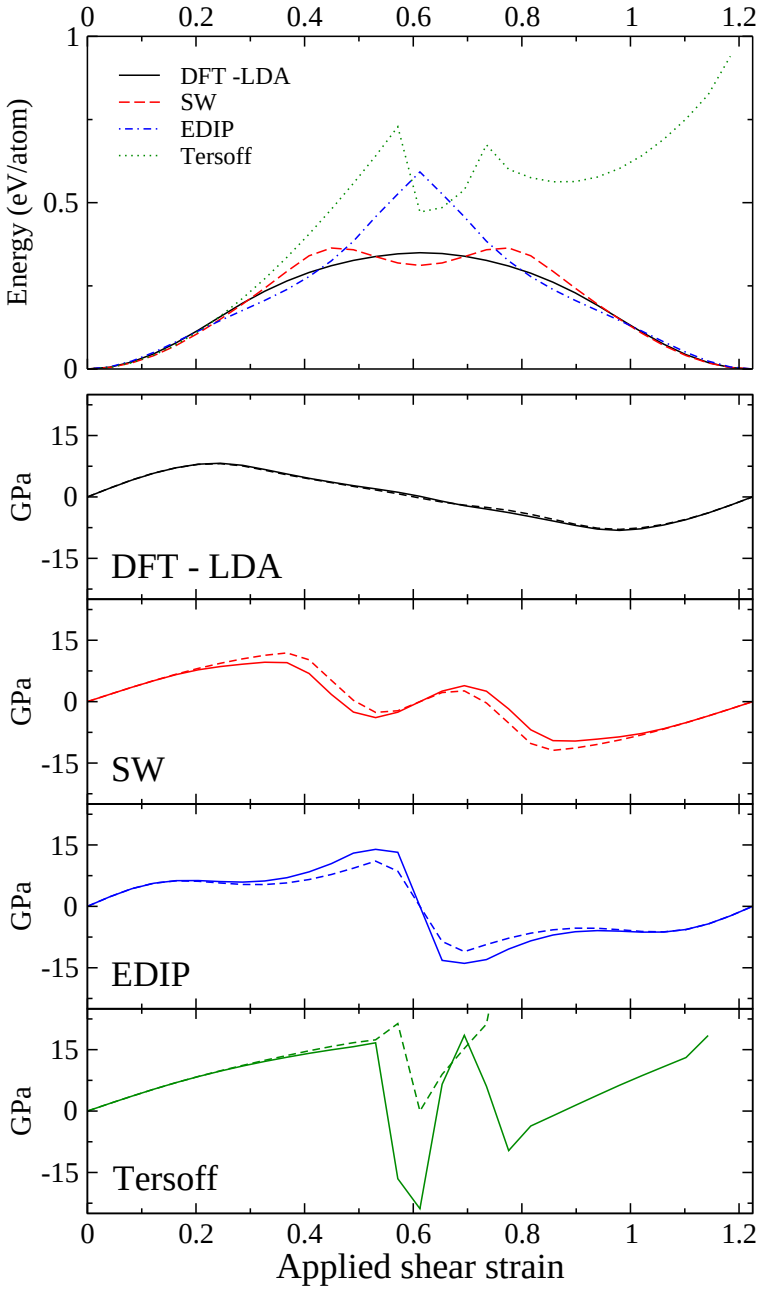
Energy (eV/atom)
DFT -LDA
SW
EDIP
Tersoff
GPa
DFT - LDA
SW
EDIP
Tersoff
Applied shear strain

Figure 3

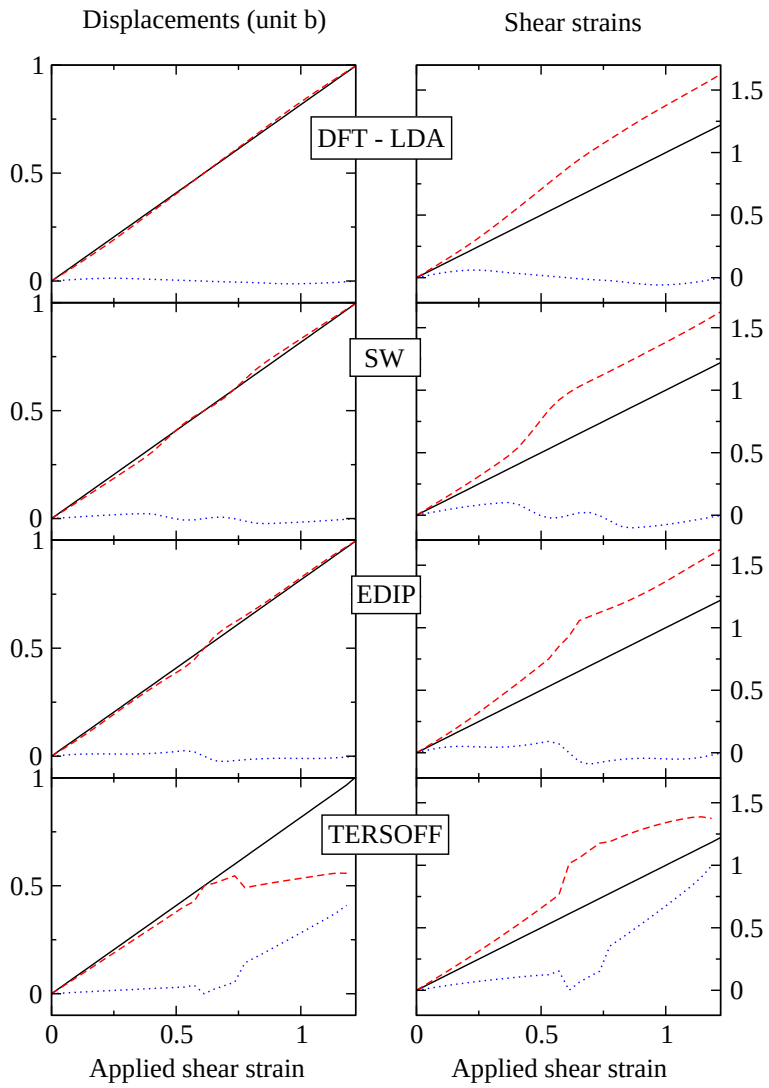
Displacements (unit b)
Shear strains
DFT - LDA
SW
EDIP
TERSOFF
Applied shear strain
Applied shear strain

Figure 4

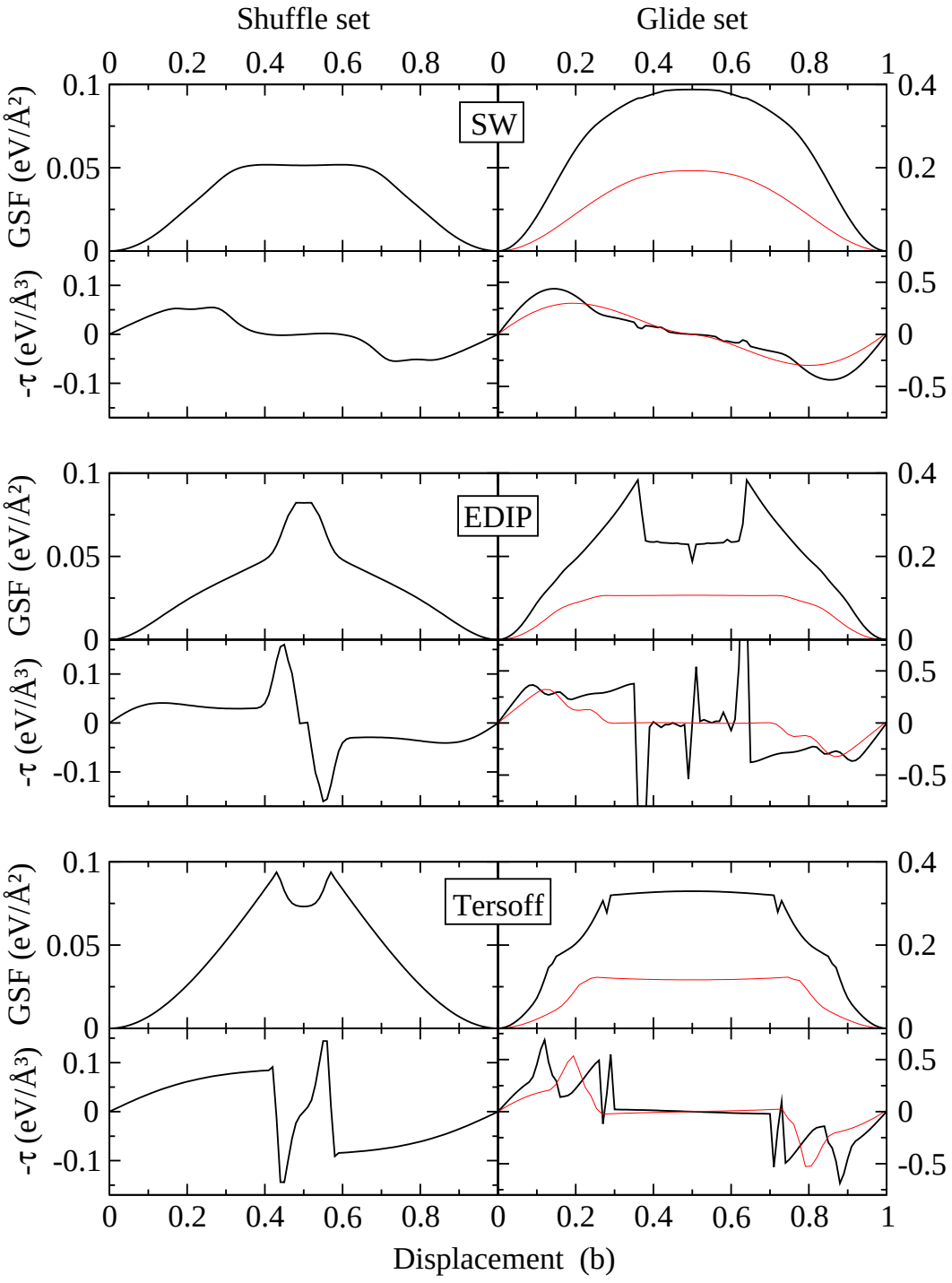
Shuffle set
Glide set
SW
EDIP
Tersoff
GSF (eV/Å²)
-τ (eV/Å³)
Displacement (b)

Figure 5